FEBS Letters 564 (2004) 340–348 FEBS 28300

An antibody library for stabilizing and crystallizing membrane proteins – selecting binders to the citrate carrier CitS

Daniela Röthlisberger[a], Klaas Martinus Pos[b], Andreas Plückthun[a,*]

[a] *Biochemisches Institut, Universität Zürich, Winterthurerstrasse 190, CH-8057 Zürich, Switzerland*
[b] *Institut für Mikrobiologie, D-BIOL, Eidgenössische Technische Hochschule, ETH-Zentrum, Schmelzbergstrasse 7, CH-8092 Zürich, Switzerland*

Received 15 December 2003; accepted 23 February 2004

First published online 1 April 2004

Edited by Fritz Winkler and Andreas Engel

Abstract Co-crystallization of membrane proteins with antibody fragments may emerge as a general tool to facilitate crystal growth and improve crystal quality. The bound antibody fragment enlarges the hydrophilic part of the mostly hydrophobic membrane protein, thereby increasing the interaction area for possible protein–protein contacts in the crystal. Additionally, it may restrain flexible parts or lock the membrane protein in a defined conformational state. For successful co-crystallization trials, the antibody fragments must be stable in detergents during the extended period of crystal growth and must be easily produced in amounts necessary for crystallography. Therefore, we constructed a library of antibody Fab fragments from a framework subset of the HuCAL GOLD® library (Morphosys, Munich, Germany). By combining the most stable and well expressed frameworks, V_H3 and $V_κ3$, with the further stabilizing constant domains, a Fab library with the desired properties was obtained in a standard phage display format. As a proof of principle, we selected binders with phage display against the detergent-solubilized citrate transporter CitS of *Klebsiella pneumoniae*. We describe efficient methods for the immobilization of the membrane protein during selection, for ELISA screening, and for BIAcore evaluation. We demonstrate that the selected Fab fragments form stable complexes with native CitS and recognize conformational epitopes with affinities in the low nanomolar range.

Key words: Antibody library; Phage display; Co-crystallization; Membrane protein

1. Introduction

Membrane proteins are involved in a large variety of biological functions, including signaling, molecular transport, electron transport and molecular interactions with soluble or other membrane-bound ligands. Furthermore, a great fraction of approved drugs act on membrane proteins, yet their molecular mechanisms of action are only poorly understood. A prerequisite for elucidating these natural and drug-induced mechanisms in detail is access to high-resolution three-dimensional structures. However, only about 75 structures of membrane proteins are currently found in the Protein Data Bank, as compared to about 23 000 structures of soluble proteins. This disparity might reflect the difficulties encountered with the production, the purification, the stability, and the crystallization of membrane proteins.

Two main limitations in the structural analysis of membrane proteins are, first, the production of sufficient amounts of pure, solubilized protein that retains its native structure and, second, the growth of highly ordered crystals with good diffraction quality. Evaluation of different expression systems and screening of homologous membrane proteins from different organisms is unavoidable for optimizing expression yield and stability. In order to obtain better ordered crystals or even to allow crystal formation at all, one approach has been successfully applied for a number of membrane proteins: co-crystallization with antibody fragments [1–7].

There appear to be two mechanisms by which an antibody fragment can aid the crystallization of membrane proteins. First, the bound antibody fragment increases the overall hydrophilicity of the complex. This enlarged hydrophilic surface contributed by the bound antibody fragment can form stable protein–protein contacts needed for crystallization. This is especially important for membrane proteins that have only short loops connecting the transmembrane helices and no extended extracellular or intracellular domains. Second, binding of the antibody fragment may stabilize one specific conformation of the membrane protein and thereby increase the structural homogeneity of the protein sample. This is particularly important for membrane proteins with highly flexible regions. In order to serve as a crystallizing ligand, the antibody fragment has to recognize an epitope that is only present in the native conformation (and not in the denatured state) of the membrane protein, bind with high affinity, and form stable and rigid complexes. As more and more effort is being invested in the structural analysis of membrane proteins, a fast and reliable system for the generation of such antibody fragments is needed.

Recombinant antibody technology offers powerful tools to quickly generate binders against a wide variety of targets [8–11]. Unlike traditional immunization of laboratory animals, recombinant antibody technology can accomplish a desired selection within a month. Moreover, the outcome is independent of the immune response of the animal, and selection conditions can be adjusted to favor the selection of

*Corresponding author. Fax: (41)-1-635 5712.
E-mail address: pluecthun@bioc.unizh.ch (A. Plückthun).

Abbreviations: V_H/V_L, variable domains of the heavy and light chain; CDR, complementary determining region; ELISA, enzyme-linked immunosorbent assay; BAD, biotin acceptor domain; BSA, bovine serum albumin; IMAC, immobilized metal ion affinity chromatography; PEG, polyethylene glycol; HRP, horseradish peroxidase; AP, alkaline phosphatase; GdnHCl, guanidine hydrochloride; K_D, equilibrium dissociation constant; PBS, phosphate-buffered saline

0014-5793/04/$30.00
doi:10.1016/S0014-5793(04)00359-X

antibodies with the above specifications. However, not all antibody fragments have biophysical characteristics suitable for co-crystallization with membrane proteins, particularly with regard to stability and expression yield. To avoid optimization of each selected antibody fragment prior to crystallization trials, the proper design of the antibody fragment library is crucial. With a fully synthetic approach, all library members can be constructed from a template that is stable, well expressed, and monomeric in solution. Here, we describe a Fab fragment library that meets these requirements.

A number of recombinant antibody formats exist. Single antibody domains from camels have been obtained and characterized [12–16] and soluble versions of human V domains have been made [17]. However, their surface areas are probably too small to favor additional crystal contacts. In addition, it remains unclear whether high affinities can be obtained with these molecules on a routine basis. Fv fragments were the first antibody fragments to be described [18], but are now rarely used because of the limited interfacial stability between heavy and light chain variable domains (V_H and V_L). Nevertheless, an Fv fragment can be stabilized in complex with its antigen and successful co-crystallization trials with membrane proteins have been reported [1–4,7]. Single-chain Fv (scFv) fragments are most popular [19–21] and quite a number of them have been crystallized with and without antigen (e.g. [22–24]). Sometimes a monomer/dimer equilibrium of scFv fragments exists, depending on the sequence of the individual antibody, and thus this format is not ideal for crystallization of difficult targets. It has been shown in a comparative evaluation of scFv and Fab fragments that the constant domains can further stabilize the variable domains in the Fab fragment (D. Röthlisberger et al., manuscript in preparation). The presence of both constant domains not only increases the interaction at the heavy and light chain interface, but they also optimally place and orient the C-terminal ends of the variable domains such that tight interface interactions are optimized. Therefore, the Fab format was chosen for the antibody library.

In recent years, several selection systems have been developed for protein–protein interactions, including cell-based systems such as the protein fragment complementation assay [25] and the yeast two-hybrid system [26], partially in vitro systems such as phage display [27] or fully in vitro systems such as ribosome display [28]. We chose phage display for the present library because the display of Fab fragments, containing two unlinked chains, is possible with this system and the selection step is performed in vitro such that a solubilized membrane protein can serve as target. Moreover, the phage particle constitutes a robust vehicle and is therefore suited for working in detergent solutions.

The principle of phage display as used for membrane proteins is illustrated in Fig. 1. DNA encoding the antibody library is cloned as a fusion to the minor coat protein gIIIp. The fusion protein is expressed and incorporated into newly produced phage particles assembled in *Escherichia coli*. The antibody fragment is thereby presented on the phage surface while its encoding gene resides within the phage genome and is packaged within the phage particle. Antibody-presenting phages are then subjected to selection, where specific phages can form complexes with the target in solution. The target/Fab fragment complexes are captured on magnetic particles, while non-binding phages are washed away. Bound phages

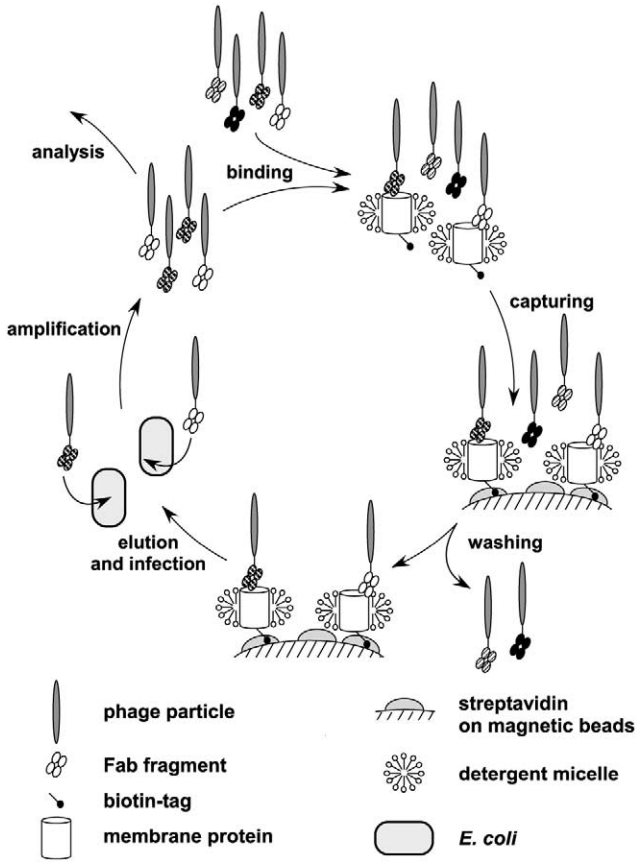

Fig. 1. Phage display cycle. A library of Fab fragments is displayed on the surface of phage particles while their genes are cloned into a phagemid, which is packaged in the phage particle. The phage library is exposed to the target molecule, the detergent-solubilized citrate carrier CitS, and phages with the desired specificities form antibody/antigen complexes. These complexes can be captured on streptavidin magnetic particles using a biotin tag present on the target molecule. Unbound phages are washed off. The remaining phages are eluted from the magnetic particles with a pH shift and used to infect host bacteria. These phages are amplified and represent in effect a sub-library, which can be used for another phage display cycle. Usually after three to five recursive cycles, single clones are selected and analyzed.

can be eluted from the immobilized complexes and used to infect *E. coli*. The physical linkage between the antibody fragment phenotype and genotype allows the amplification of specific antibody fragments displayed on the phage surface. The recovered clones can initiate a new selection cycle or be further analyzed in detail.

To check the performance of the newly assembled library, we used the citrate carrier CitS, a secondary transporter from *Klebsiella pneumoniae*, as a model membrane protein. It is thought that especially for transporters, which normally do not possess extensive hydrophilic domains, the binding of antibody fragments will enhance the formation of protein–protein contacts. CitS is biochemically well-characterized [29–32] and has an experimentally determined membrane topology of 11 transmembrane segments [33]. It can be produced in sufficient amounts [34,35], and is functional after reconstitution into liposomes [30]. This makes CitS a suitable model membrane protein to establish a system for fast and reliable selection of antibody fragments used in co-crystallization trials.

2. Materials and methods

2.1. Protein expression and purification

The citrate carrier CitS from *K. pneumoniae* was expressed with either an N-terminal His_{10} tag or a C-terminal biotin acceptor domain (BAD) fusion and purified as described [35]. The biotinylated CitS fusion consists of full-length CitS (GenBank/EMBL Data Bank, accession number M83146, aa 1–446) directly fused to BAD of oxaloacetate decarboxylase from *K. pneumoniae* (GenBank/EMBL Data Bank, accession number J03885, aa 491–595). The gene encoding biotin ligase, *birA*, was co-expressed from the same plasmid (pMalccit-SabirA [35]) in *E. coli* DH5α [36]. For the His-tagged version, which contains two factor Xa cleavage sites in series, the amino acid sequence M-G-$(H)_{10}$-S-S-G-H-I-E-G-R-H-M-L-D-R-G-S-I-E-G-R was fused to the first amino acid of CitS in the vector pET16b (Novagen [30]). The His-tagged version was expressed in *E. coli* C43(DE3) [37]. After purification, CitS was desalted with a PD-10 column (Amersham Biosciences) to remove biotin or imidazole. Protein concentrations were determined by the D_C protein assay (Bio-Rad) using bovine serum albumin (BSA) as a standard.

The selected Fab fragments were cloned into the expression plasmid pMx9 [38], where a mycHis$_5$ tag was introduced at the C-terminus of the heavy chain. Expression and purification of soluble Fab fragments was essentially performed as described [39] with the exception that cultures were grown in SB medium (20 g tryptone, 10 g yeast extract, 5 g NaCl per liter) and induced at an OD_{600} of 0.5–0.6. The Fab fragments were purified on tandem columns (IMAC/HQ) operated by a BioCAD system. In this strategy, the eluate from the IMAC column, which exploits the C-terminal His tag, was directly loaded onto a HQ anion exchange column in 10 mM Tris, pH 7.5. The Fab fragments were recovered in the flow-through, while the contaminating proteins remained bound to the HQ column. Protein concentrations were determined by measuring the absorbance at 280 nm using the calculated extinction coefficient [40].

2.2. Phage display

In the selection procedure, about 10^{11} phages representing the Fab fragment library were incubated with 100 nM of biotinylated citrate carrier CitS in 100 μl CitS buffer (20 mM potassium phosphate, pH 7.0, 500 mM NaCl, 20% glycerol, 0.1% dodecylmaltoside) for 1 h at 4°C. Two independent selections were performed in each round, one in the absence of citrate and one in the presence of 1 mM citrate. The complexes were captured with 150 μl streptavidin magnetic particles (Roche) and washed 10 times with 1 ml CitS buffer at 4°C. Bound phages were eluted with 100 μl of 100 mM glycine, pH 2.2 and then neutralized with 100 μl of 1 M Tris, pH 8.0. *E. coli* TG1 cells [41] (5 ml, $OD_{600} = 0.8$) were infected with the pH-neutralized phages and then plated on large LB agar plates containing 30 μg/ml chloramphenicol and 1% glucose. The plates were incubated overnight at 37°C and the cells were scraped off the next day to inoculate 100 ml of 2×TY (16 g tryptone, 10 g yeast extract, 5 g NaCl per liter) containing 30 μg/ml chloramphenicol and 1% glucose. The culture was incubated at 37°C and at an $OD_{600} = 0.5$ the phage library was rescued by infection with VCS M13 helper phage (Stratagene; multiplicity of infection ~20). The cells were harvested and resuspended in 150 ml 2×YT containing 30 μg/ml chloramphenicol and 50 μg/ml kanamycin and grown overnight at 30°C for phage production. The phages were precipitated from the culture supernatant with 25 ml polyethylene glycol (PEG) solution (20% PEG 6000, 2.5 M NaCl) and redissolved in 1 ml of high salt phosphate-buffered saline (PBS; 20 mM potassium phosphate, pH 7.0, 500 mM NaCl). After the fourth round, 30 clones (15 clones from the selection in the presence and 15 clones from the selection in the absence of 1 mM citrate) were randomly picked and analyzed by enzyme-linked immunosorbent assay (ELISA), and the positive clones were sequenced.

2.3. ELISA

For a first screening, phage ELISA with single Fab fragments displayed on the phage surface was performed. A Maxisorp plate (Nunc) was coated with neutravidin (Pierce, 66 nM in PBS) overnight and blocked for 2 h with 3% BSA in PBS at 4°C. All subsequent incubations and washes were performed in CitS buffer at 4°C. Biotinylated citrate carrier CitS (0.27 μM) was immobilized by incubation for 1 h. About 10^9 phages displaying selected single clones were preincubated with either buffer (for the binding signal) or 0.27 μM His-tagged, non-biotinylated CitS (for the specific inhibition of binding signal) for 1 h on ice and then added to the immobilized CitS. Bound phages were incubated with anti-M13 antibody horseradish peroxidase (HRP) conjugate (Amersham Pharmacia Biotech) and detected with a subsequent color reaction (soluble BM blue POD substrate, Roche Diagnostics). The color reaction was stopped by adding 1 M HCl to the sample and the absorbance was measured at 450 nm with an HTS 7000 Plus plate reader (Perkin Elmer).

For the characterization of positive single clones, ELISA in the Fab format was performed. Fab fragments (500 nM in PBS) were directly coated on a Maxisorp plate (Nunc) overnight at 4°C. The plate was blocked with 3% BSA in PBS for 2 h at 4°C. All subsequent incubations and washes were performed in CitS buffer at 4°C. Biotinylated CitS (100 nM) was preincubated with increasing amounts of the same Fab fragment as immobilized in the well (0–1 μM) for 1 h on ice and then added to the well for 1 h. CitS bound to the Fab fragment was detected with streptavidin–alkaline phosphatase (AP) conjugate (Roche) in a subsequent color reaction (1.1 mg/ml 4-nitrophenyl phosphate (Fluka) in 100 mM Tris, pH 8.8, 100 mM NaCl, 5 mM $MgCl_2$) by measuring the absorbance at 405 nm with an HTS 7000 Plus plate reader (Perkin Elmer).

2.4. Equilibrium denaturation measurements

The unfolding of the Fab fragments was followed by the shift of the emission maximum or the intensity at 330 or 350 nm at each denaturant concentration using fluorescence spectroscopy. All fluorescence measurements were performed with a PTI Alpha Scan spectrofluorimeter (Photon Technologies) using an excitation wavelength of 280 nm and recording the emission spectra between 320 nm and 365 nm. The protein concentration was 0.2 μM in all experiments. The Fab fragments were incubated for 1 day at 20°C in PBS (20 mM potassium phosphate, pH 7, 150 mM NaCl) containing varying amounts of guanidine hydrochloride (GdnHCl). We chose this incubation time arbitrarily, as a slow unfolding of the Fab fragment was reported previously [42,43]. The exact denaturant concentration in each sample was determined from its refractive index.

2.5. Determination of dissociation constants by competition BIAcore

Competition BIAcore analysis [44,45] was performed under conditions of mass transport limitation using a CM5 sensor chip (BIAcore) coated with 2200–2400 resonance units of Fab fragment, immobilized by amine coupling. The CM5 surface was used as a background control. Biotinylated CitS was preincubated with different concentrations of Fab fragments, acting as competitor of binding, for at least 1 h prior to injection, and the mass transport-limited rate was measured as a function of Fab fragment concentration. Each binding–regeneration cycle was performed at 10°C with a constant flow rate of 20 μl/min in 20 mM potassium phosphate, pH 7.0, 500 mM NaCl, 10% glycerol, 0.1% dodecylmaltoside. In each cycle, buffer (50 μl) was injected first to stabilize the baseline, followed by sample injection (200 μl), and then 20 μl glycine (50 mM, pH 3) and 20 μl 5 M NaCl were used for regeneration. Data were processed with the software Scrubber (D. Myszka, University of Utah, http://www.cores.utah.edu/Interaction/software.html) and evaluated with BIAevaluation (BIAcore). The slopes of the mass transport-limited rate (r_{obs}) during injection [44,45] were plotted against total Fab fragment concentrations to fit the dissociation constant using Eq. 1 [46]:

$$r_{obs} = r_{max} \cdot \left(1 - \frac{1}{[CitS]_{tot}} \cdot \left(\frac{K_D + [Fab]_{tot} + [CitS]_{tot}}{2} - \sqrt{\left(\frac{K_D + [Fab]_{tot} + [CitS]_{tot}}{2}\right)^2 - [CitS]_{tot} \cdot [Fab]_{tot}}\right)\right) + \text{offset} \quad (1)$$

where r_{obs} is the slope at a given $[Fab]_{tot}$, r_{max} is the maximal slope in the absence of inhibition, $[CitS]_{tot}$ is the total CitS concentration, $[Fab]_{tot}$ is the total Fab fragment concentration, and K_D is the dissociation constant.

2.6. Size exclusion chromatography

Biotinylated CitS fusion protein was incubated with Fab fragment present in molar excess for 1 h on ice. Samples (100 μl) of free and complexed CitS solution were each applied on a Superdex 200 column (Amersham Biosciences) and the elution profiles were monitored by absorbance at 280 nm and 230 nm.

2.7. Western blot

His-tagged CitS, myc-tagged Fab fragment and prestained protein marker (broad range; New England Biolabs) were subjected to sodium dodecyl sulfate–polyacrylamide gel electrophoresis (SDS–PAGE) and Western blot analysis using an Immobilon™-P membrane (Millipore). The membrane was blocked with 5% milk in PBS and incubated with 1 μM myc-tagged Fab fragment in 1% milk/PBS for 1 h at room temperature. To detect Fab fragments bound to the blotted CitS, the membrane was incubated with anti-myc antibody 9B11 (1:1000 in 1% milk/PBS; Cell Signaling Technology) followed by anti-mouse antibody AP conjugate (1:10 000 in 1% milk/PBS; Sigma) for 1 h at room temperature. Bound antibodies were detected by a precipitating color reaction with 5-bromo-4-chloro-indolyl-phosphate toluidine salt (150 μg/ml; Fluka) and nitroblue tetrazolium (37.5 μg/ml; Fluka) in 100 mM Tris, pH 8.8, 100 mM NaCl, 5 mM $MgCl_2$.

3. Results

3.1. Library construction

Two biophysical features of antibody fragments are considered to be most critical for successful co-crystallization of membrane proteins. These are first the production of antibody fragments in quantities sufficient for co-crystallization trials and second high thermodynamic stability to ensure that the antibody fragment remains folded in detergent solution during both selection and crystal growth. To achieve the best biophysical behavior of antibody fragments, both the format and the framework used in the synthetic antibody fragment library have to be optimally designed prior to selection against solubilized membrane proteins.

For reasons explained in detail in Section 1, we chose the Fab format for this purpose. Since the yields obtained with Fab fragments are frequently lower than with the corresponding scFv fragments [9], we decided to limit the library to variable domains with the best overall biophysical properties. The choice of the antibody framework is based on a systematic evaluation of the biophysical properties of isolated human consensus variable domains, derived from HuCAL® [47], and V_H/V_L combinations thereof [39]. Ewert et al. [39] have analyzed and compared the expression behavior, oligomeric state in solution, and thermodynamic stability of all constructs. A very strong correlation between the properties of the isolated domains and their combination in the scFv fragment has been found. This previous work has shown that $V_H3/V_κ3$ is the most favorable scFv fragment with superior properties: the scFv fragment as well as the isolated V_H3 and $V_κ3$ domains show high thermodynamic stability and good expression yield. The $V_H3/V_κ3$ scFv fragment is monomeric in solution and behaves well under all circumstances [39].

We therefore decided to create a $V_H3/V_κ3$ single framework phage display library in the Fab format. As a starting point we used the HuCAL GOLD® Fab library (Morphosys, Munich, Germany). While it contains consensus frameworks as in the original HuCAL® design [47], the most important modification in the HuCAL GOLD® library is that all six complementary determining regions (CDRs) have been diversified (S. Urlinger, C. Rothe et al., Morphosys, unpublished). While CDR-H3 and CDR-L3 are varied as previously described [47], CDR1 and CDR2 in both heavy and light chains are diversified in a structure-guided approach, in order to keep structural anchor positions intact and to statistically bias the library towards residues typically found in rearranged sequences. This was achieved using trinucleotide codons [48] in the gene synthesis. While the HuCAL GOLD® library uses a disulfide link between the Fab fragment and gIIIp of the phage [49], in the present library, the heavy chain has been fused directly to gIIIp, as usually done in phage display [38,50,51]. For applications in crystallography, achieving the best possible biophysical properties throughout the library is more important than maximal diversity, and it is for this reason that we decided to use only a subset of frameworks, namely V_H3 and $V_κ3$. About 3×10^8 independent clones were obtained after transformation of the ligated library. Sequence analysis of 30 unselected clones showed that, as in the starting HuCAL GOLD® library, the diversity and length distribution of the CDRs corresponded to the design. Ninety percent of all sequenced clones were still in-frame and contained no stop codon, yielding a high-quality library with a functional size of 2.7×10^8.

3.2. Selection using phage display

To select conformation-specific Fab fragments, the membrane protein has to be in its native conformation. Selection on whole cells [52–55] is one possibility to achieve this goal, since the membrane protein remains in its natural environment guaranteeing its structural integrity. However, whole cells represent a very complex antigen source, which can complicate the selection procedure or even make it impossible, if the membrane protein in question is not well accessible, or if the expression level is too low [56,57]. Furthermore, only extracellular epitopes can be targeted. Therefore, pure membrane proteins are required to accelerate and simplify the selection procedure. After solubilization and purification the membrane protein can be used directly (this paper) or reconstituted into proteoliposomes [58,59] prior to selection. In the reconstituted state the biological activity of the membrane protein can be measured to ensure the native conformation of the membrane protein. In addition, the detergent problem is eliminated as it is often a problem to keep the membrane protein stable in detergent for a long time. However, this procedure is more time-consuming than direct selection on solubilized membrane protein and, depending on the method used, can lead to oriented insertion of the membrane proteins [60–62], which again hides half of the potential binding surface and makes even the exposed surface less accessible. Furthermore, for some membrane proteins the biological activity can also be assessed in the detergent-solubilized state [63–68]. Most importantly for the application in structural studies, in panning experiments with the solubilized membrane protein, the selection is performed under the same condition as the crystallization procedure, which ensures a good performance of the Fab fragments during co-crystallization.

A unique problem in the selections involving solubilized membrane proteins is their immobilization whilst keeping them in a native conformation in detergent solution. Direct immobilization on polystyrene would most probably not re-

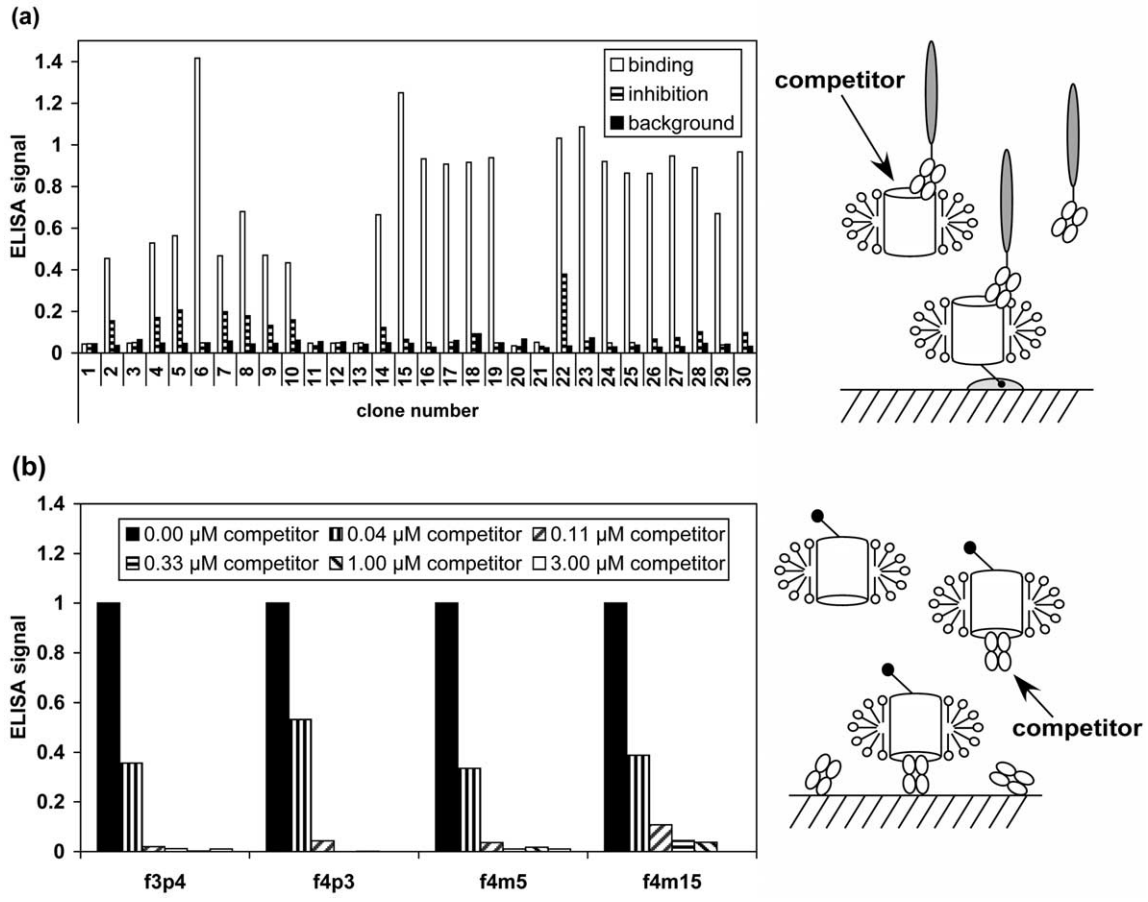

Fig. 2. ELISA assays to test the specificity of selected clones. a: The initial screening for specific binders is shown with a scheme of the experimental set-up. The binding of single phages, displaying the Fab fragments, to immobilized CitS (binding) or neutravidin (background) was examined. The binding to immobilized CitS can be inhibited with free antigen as competitor (inhibition). In a subsequent ELISA the functionality of the free Fab fragments was tested (b). The binding of CitS to the immobilized Fab fragment was inhibited with increasing amounts of free Fab fragment.

tain the membrane protein in its native conformation, while immobilization with peptide tags can become significantly weakened in detergent or lead to strong non-specific binding (D. Ott et al., unpublished). Therefore, we initially evaluated in this work the efficacy of several tags in the presence and absence of 0.1% dodecylmaltoside in an ELISA format to ensure that buffer conditions do not interfere with binding (data not shown). The detection of biotin with streptavidin–AP conjugate (Roche Diagnostics), myc tag with 9B11 antibody (Cell Signaling Technology), FLAG tag with M2 antibody (Sigma) and His tag with anti-tetra-His antibody (Qiagen) were tested, and all bound antibodies were detected with an anti-mouse IgG–AP conjugate (Sigma). For subsequent screening, we additionally tested an anti-M13–HRP conjugate (Roche Diagnostics) that recognizes the major coat protein gVIIIp of bacteriophage M13. In this comparison, the anti-M13–HRP conjugate performed best. For biotin and myc tag detection the signal in detergent reaches about half the signal in buffer, and is still clearly detectable over background signal. Relatively high background signals were observed for FLAG tag detection in detergent, and the His tag detection gives only weak signals compared to the other detection systems. Therefore, we chose to use an enzymatically added biotin moiety for membrane protein immobilization.

After four rounds of selection, 30 phage clones (15 clones either in the presence or absence of citrate during selection, see Section 2) were isolated and screened for binding to CitS by ELISA (Fig. 2a). To test the specificity the binding was inhibited using the His-tagged version of CitS. Positive clones (77% of all screened clones) were sequenced. Four different

Table 1
Summary of biophysical characterization of the selected Fab fragments

Clone	Yield (mg/l culture)	Midpoint of unfolding (M)	K_D (nM)
f3p4	3.1	2.0	4 ± 2
f4p3	1.2	2.2	n.d.
f4m5	2.5	1.5	n.d.
f4m15	1.7	1.6	27 ± 7

n.d., not determined.

(a)

	framework 1	CDR 1	framework 2	CDR 2	framework 3	CDR 3	framework 4
clone f3p4		G F T F R N S A M H		W V S S I W Y S G S N T Y Y A D S V K G		F A G G W G A Y D V	
clone f4p3		G F T F R N S A M H		W V S S I W Y S G S N T Y Y A D S V K G		F A G G W G A Y D V	
clone f4m5		G F T F R N S A M H		L V S G I V Y S G S S T Y Y A D S V K G		G N S Y G H D T F D V	
clone f4m15		G F T F R N Y A M S		W V S A I S Y S S S N T Y Y A D S V K G		D Q D Y E G G Y D F	

(b)

	framework 1	CDR 1	framework 2	CDR 2	framework 3	CDR 3	framework 4
clone f3p4		R A S Q S V S S N Y L A		Y D S S S R A T		H Q Y S D I S P	
clone f4p3		R A S Q S L S S S L A		Y Q A S S R A T		Q Q Y G S V P Y	
clone f4m5		R A S Q S L S S S L A		Y Q A S S R A T		Q Q Y G S V P Y	
clone f4m15		R A S Q I G D S N Y L A		G G A S S R A T		Q Q Y G G I P P	

Fig. 3. The CDR sequences of the selected clones are shown, while the consensus sequences of the framework regions are as described for V_H3 and V_K3 [47]. Panel a represents CDR1 to CDR3 of the heavy chain and panel b CDR1 to CDR3 of the light chain.

sequences were identified (Fig. 3), three independent clones and one clone (f4p3) which share the H-CDRs from clone f3p4 and the L-CDRs from clone f4m5. No specific enrichment of particular clones was observed for the selection in the presence or absence of citrate.

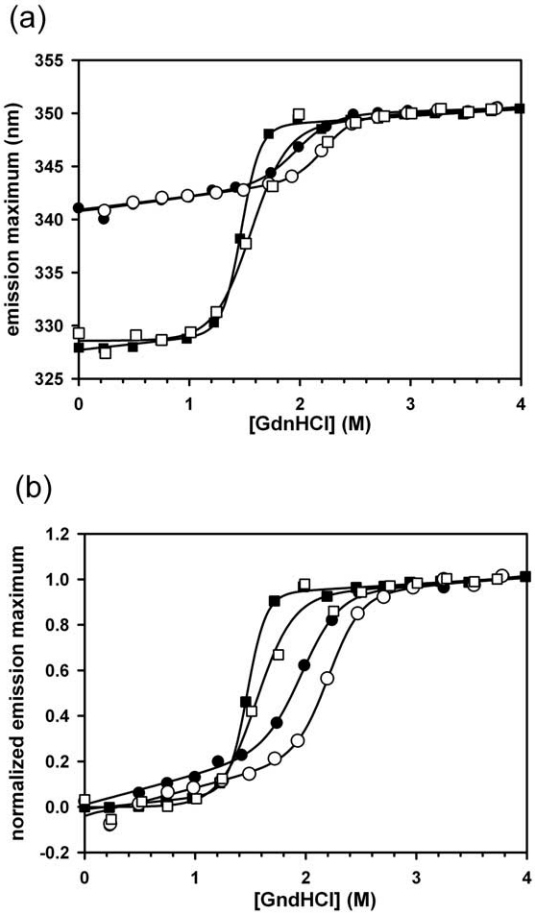

Fig. 4. Overlay of guanidine-induced unfolding curves of the selected Fab fragments. Unfolding was followed by the change in emission maximum as a function of denaturant concentration at an excitation wavelength of 280 nm. Clones f3p4 (●) and f4p3 (○) have three tryptophans in the CDR loops, compared to only one tryptophan for f4m15 (□) or none for f4m5 (■). Therefore the emission maximum of the first two is red-shifted in the native state to about 341 nm (a), as these tryptophans are already solvent-exposed. For better comparison of the midpoints of unfolding, the curves are normalized (b), with the emission maximum at 0 M GdnHCl as 0 and the emission maximum at 4 M GdnHCl as 1. Note that this normalization makes no assumption about the pre- and post-transition baselines.

3.3. Biophysical behavior of selected clones

Routinely, between 2 and 3 mg of pure periplasmically produced Fab fragment was obtained after a two-column purification from a non-optimized standard 1 l *E. coli* shake-flask culture. Only clone f4p3 was expressed at a slightly lower level (about 1.2 mg of pure protein) (Table 1). It should be mentioned that for reasons of speed, small IMAC columns with high loading rates were used, leaving room for significant yield improvements. Guanidine-induced equilibrium unfolding curves were measured for all four selected clones (Fig. 4). Because of the four-domain structure of the Fab fragment the unfolding is unlikely to be a two-state process, although a steep transition is observed in all cases. We therefore did not determine ΔG values but compared the midpoints of unfolding as a semiquantitative measure of stability. The midpoints of unfolding lie between 1.5 M and 2.2 M GdnHCl (Table 1), consistent with these Fab fragments being highly stable proteins.

3.4. Specificity and affinity

To analyze the binding properties of the isolated Fab fragments, we immobilized each Fab fragment directly to the well, and detected binding of biotinylated CitS to the Fab fragment with streptavidin–AP fusions. Binding of CitS was observed to the immobilized selected Fab fragments (Fig. 2b), but not

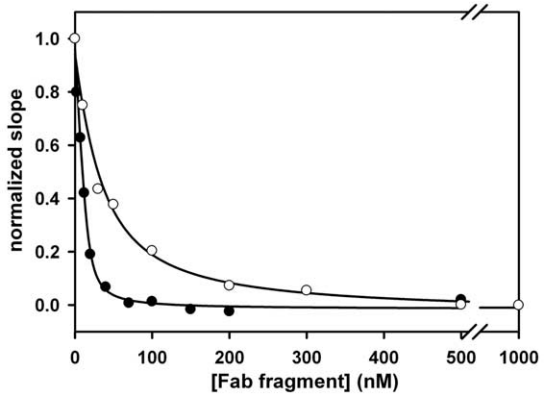

Fig. 5. Determination of the equilibrium dissociation constants K_D. Purified CitS was mixed with different concentrations of Fab fragments and incubated for at least 1 h on ice before analysis. Samples were injected over the sensor chip coated with the corresponding Fab fragment. The normalized slopes were plotted against the corresponding concentration of soluble Fab fragment. The slopes correlate to the amount of uncomplexed CitS. From a fit with Eq. 1 (solid line), K_D was calculated. The fitted lines correspond to K_D of 4 ± 2 nM for the Fab fragment f3p4 (●) and 27 ± 7 nM for the Fab fragment f4m15 (○).

to neutravidin or to an unrelated Fab fragment. Furthermore, increasing amounts of free Fab fragment in solution inhibited binding of CitS to the immobilized Fab fragment. This demonstrates that all selected Fab fragments specifically recognize CitS. Using the same set-up, we also observed that all Fab fragments compete with each other for binding, indicating that the Fab fragments bind to the same epitope or overlapping epitopes on the CitS molecule.

To determine the dissociation constants of the binders, competition BIAcore was performed. The Fab fragments were covalently linked to the CM5 chip by amine coupling. Because the Fab fragments were more stable against buffer changes than the membrane protein, this allowed for a rapid and easy regeneration procedure using low pH and high salt washes. In contrast to ELISA, BIAcore measurements do not rely on tags or markers. Therefore, we were able to cross-check the determined affinity constants with both CitS variants, either the N-terminal His_{10} tag or the C-terminal BAD fusion protein. We determined the equilibrium dissociation constants for two binders, and both Fab fragments showed high affinities with K_D values in the low nanomolar range (Fig. 5) and no differences in binding affinities to the two CitS variants were observed (data not shown).

3.5. Complex formation

The tight interaction between CitS and the Fab fragment was also demonstrated by gel filtration chromatography. Stable CitS/Fab fragment complexes were formed and eluted in a single peak (Fig. 6). For comparison, the elution profiles of the free biotinylated CitS (Fig. 6, dashed line) and the complex with molar excess of Fab fragment (Fig. 6, solid line) are shown. A clear shift towards higher molecular weight is observed for the CitS/Fab fragment complex as compared to free CitS. The SDS–PAGE analysis of the high molecular weight peak clearly shows the presence of both CitS and the Fab fragment (Fig. 6, inset). It can be concluded that the selected Fab fragments bind to CitS in its detergent-solubilized conformation. Moreover, when the binding of the Fab fragments was tested against SDS–PAGE-denatured CitS by Western blot analysis, none of the selected Fab fragments was able to detect CitS (Fig. 7). This indicates that the selected Fab fragments bind to a conformational epitope.

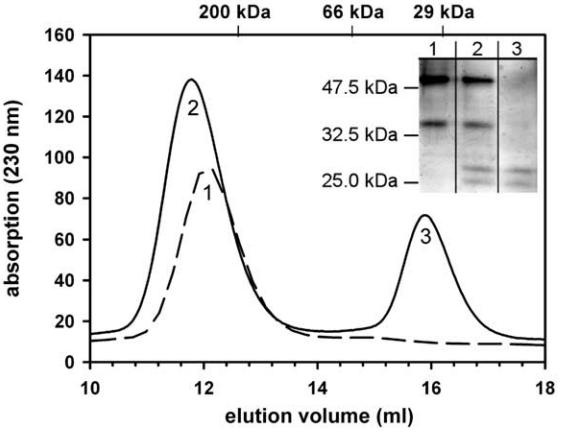

Fig. 6. Overlay of gel filtration elution profiles. Free biotinylated CitS (dashed line) and biotinylated CitS mixed with excess Fab fragment f4m5 (solid line) were loaded onto a Superdex 200 column. The CitS/f4m5 complex is shifted towards higher molecular weight (peak 2) as compared to free CitS (peak 1). A molar mass between 45 kDa and 50 kDa was determined for the Fab fragment (peak 3) with multi-angle static light scattering (data not shown), despite its somewhat retarded elution. The corresponding peak fractions were analyzed on silver-stained polyacrylamide gel (inset). Lane 1: biotinylated CitS peak. The smaller molecular weight band corresponds to CitS without BAD [34]. Lane 2: CitS/Fab fragment complex peak. Lane 3: Fab fragment f4m5 peak. The two bands correspond to the heavy and the light chain of the Fab fragment.

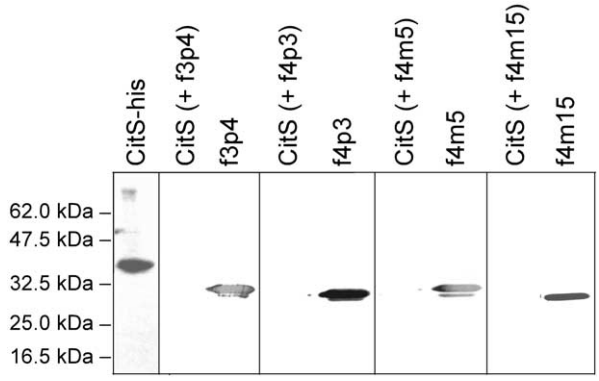

Fig. 7. Test of conformation-specific binding. His-tagged CitS was subjected to SDS–PAGE and Western blot analysis. The selected myc-tagged Fab fragments were detected with anti-myc antibody. No binding of the Fab fragments to the denatured CitS was observed. As a positive control, each corresponding myc-tagged Fab fragments was subjected to SDS–PAGE and Western blot analysis as well. For comparison, a Coomassie-stained gel of purified CitS is shown on the left hand side with the molecular weight marker indicated.

4. Discussion

Recombinant antibody technology provides a powerful tool for selecting particular antibody fragments that have the desired specificity and functionality from billions of potentially binding molecules [8–11]. This universally applicable technology is also promising for the selection of crystallizing ligands for membrane proteins. A major advantage of selection techniques in which the binding step occurs in vitro is that the selection conditions can be varied and adapted to the problem (for a review of selection strategies see [69]). Selection pressure and stringency can then be adjusted to generate optimal binding molecules.

As discussed in previous studies [47,69–71] the library size and quality and the biophysical properties of the library members are all crucial for success when working with difficult targets or special applications. In order to apply antibody fragments in co-crystallization experiments with membrane proteins, the antibody fragments must be stable to remain folded in detergent solution. Furthermore, rather large amounts of protein are needed, necessitating good expression properties. Therefore, based on prior analysis and design of frameworks [39] and CDRs [47] (S. Urlinger, C. Rothe et al., Morphosys, unpublished results), we assembled from a subset of HuCAL GOLD® an antibody library in the Fab phage format whose members have these desired properties. This high-quality library has a functional size of 2.7×10^8 independent clones. The favorable biophysical properties engineered into the library guarantee that functionality is maintained during selection.

We have demonstrated that all selected clones possess the required characteristics. For crystallization, several milligrams

of protein are needed, which is now easily achieved from shake-flask cultures. This is an advantage because many antibody fragments show poor expression behavior, especially if derived from immunized laboratory animals [72]. In equilibrium unfolding experiments, the thermodynamic stabilities of the selected Fab fragments were measured and the observed range of stability corresponds well to other stability-engineered or selected antibody fragments [73–75].

Although the library members fulfill all basic biophysical requirements, the binding mode of the antibody fragment to the membrane protein is also important for successful co-crystallization. An affinity in the low nanomolar range, as determined for two of the CitS binders, ensures tight interaction between the antibody fragment and the membrane protein. Analysis of antibody–antigen complex formation in gel filtration and Western blot experiments revealed that all selected Fab fragments recognize a conformational epitope. All of these binding features together ensure the formation of stable and rigid complexes. This constitutes a good starting point for crystallization trials.

In summary, a Fab fragment library was assembled, in which all members display the biophysical properties desirable for co-crystallization with membrane proteins. Using phage display, a fast selection system was established for generating Fab fragments suitable for co-crystallization. For CitS, three independent clones with high affinities for conformational epitopes were selected, making further affinity or stability maturation unnecessary.

Acknowledgements: The authors thank Casim Sarkar and Dave Zechel for critical reading of the manuscript, Morphosys AG (Munich, Germany) for providing V_H3 and $V_\kappa3$ libraries and constructive collaboration on HuCAL®, and David Myszka for providing the software Scrubber.

References

[1] Iwata, S., Ostermeier, C., Ludwig, B. and Michel, H. (1995) Nature 376, 660–669.
[2] Ostermeier, C., Harrenga, A., Ermler, U. and Michel, H. (1997) Proc. Natl. Acad. Sci. USA 94, 10547–10553.
[3] Harrenga, A. and Michel, H. (1999) J. Biol. Chem. 274, 33296–33299.
[4] Hunte, C., Koepke, J., Lange, C., Rossmanith, T. and Michel, H. (2000) Struct. Fold. Des. 8, 669–684.
[5] Zhou, Y., Morais-Cabral, J.H., Kaufman, A. and MacKinnon, R. (2001) Nature 414, 43–48.
[6] Dutzler, R., Campbell, E.B. and MacKinnon, R. (2003) Science 300, 108–112.
[7] Lange, C. and Hunte, C. (2002) Proc. Natl. Acad. Sci. USA 99, 2800–2805.
[8] Winter, G., Griffiths, A.D., Hawkins, R.E. and Hoogenboom, H.R. (1994) Annu. Rev. Immunol. 12, 433–455.
[9] Plückthun, A. et al. (1996) in: Antibody Engineering (McCafferty, J., Hoogenboom, H.R. and Chiswell, D.J., Eds.), IRL Press, Oxford.
[10] Winter, G. (1998) FEBS Lett. 430, 92–94.
[11] Schaffitzel, C., Hanes, J., Jermutus, L. and Plückthun, A. (1999) J. Immunol. Methods 231, 119–135.
[12] Hamers-Casterman, C., Atarhouch, T., Muyldermans, S., Robinson, G., Hamers, C., Songa, E.B., Bendahman, N. and Hamers, R. (1993) Nature 363, 446–448.
[13] Arbabi Ghahroudi, M., Desmyter, A., Wyns, L., Hamers, R. and Muyldermans, S. (1997) FEBS Lett. 414, 521–526.
[14] Lauwereys, M., Arbabi Ghahroudi, M., Desmyter, A., Kinne, J., Holzer, W., De Genst, E., Wyns, L. and Muyldermans, S. (1998) EMBO J. 17, 3512–3520.
[15] Muyldermans, S. (2001) J. Biotechnol. 74, 277–302.
[16] Ewert, S., Cambillau, C., Conrath, K. and Plückthun, A. (2002) Biochemistry 41, 3628–3636.
[17] Holt, L.J., Herring, C., Jespers, L.S., Woolven, B.P. and Tomlinson, I.M. (2003) Trends Biotechnol. 21, 484–490.
[18] Skerra, A. and Plückthun, A. (1988) Science 240, 1038–1041.
[19] Bird, R.E. et al. (1988) Science 242, 423–426.
[20] Huston, J.S. et al. (1988) Proc. Natl. Acad. Sci. USA 85, 5879–5883.
[21] Glockshuber, R., Malia, M., Pfitzinger, I. and Plückthun, A. (1990) Biochemistry 29, 1362–1367.
[22] Ay, J., Keitel, T., Kuttner, G., Wessner, H., Scholz, C., Hahn, M. and Höhne, W. (2000) J. Mol. Biol. 301, 239–246.
[23] Boehm, M.K. et al. (2000) Biochem. J. 346, 519–528.
[24] Kaufmann, M., Lindner, P., Honegger, A., Blank, K., Tschopp, M., Capitani, G., Plückthun, A. and Grütter, M.G. (2002) J. Mol. Biol. 318, 135–147.
[25] Pelletier, J.N., Arndt, K.M., Plückthun, A. and Michnick, S.W. (1999) Nat. Biotechnol. 17, 683–690.
[26] Fields, S. and Song, O. (1989) Nature 340, 245–246.
[27] Smith, G.P. (1985) Science 228, 1315–1317.
[28] Hanes, J. and Plückthun, A. (1997) Proc. Natl. Acad. Sci. USA 94, 4937–4942.
[29] Lolkema, J.S., Enequist, H. and van der Rest, M.E. (1994) Eur. J. Biochem. 220, 469–475.
[30] Pos, K.M. and Dimroth, P. (1996) Biochemistry 35, 1018–1026.
[31] Kästner, C.N., Prummer, M., Sick, B., Renn, A., Wild, U.P. and Dimroth, P. (2003) Biophys. J. 84, 1651–1659.
[32] Sobczak, I. and Lolkema, J.S. (2003) Biochemistry 42, 9789–9796.
[33] van Geest, M. and Lolkema, J.S. (2000) Biochim. Biophys. Acta 1466, 328–338.
[34] Pos, K.M., Bott, M. and Dimroth, P. (1994) FEBS Lett. 347, 37–41.
[35] Kästner, C.N., Dimroth, P. and Pos, K.M. (2000) Arch. Microbiol. 174, 67–73.
[36] Woodcock, D.M. et al. (1989) Nucleic Acids Res. 17, 3469–3478.
[37] Miroux, B. and Walker, J.E. (1996) J. Mol. Biol. 260, 289–298.
[38] Rauchenberger, R. et al. (2003) J. Biol. Chem. 278, 38194–38205.
[39] Ewert, S., Huber, T., Honegger, A. and Plückthun, A. (2003) J. Mol. Biol. 325, 531–553.
[40] Gill, S.C. and von Hippel, P.H. (1989) Anal. Biochem. 182, 319–326.
[41] Carter, P., Bedouelle, H. and Winter, G. (1985) Nucleic Acids Res. 13, 4431–4443.
[42] Rowe, E.S. (1976) Biochemistry 15, 905–916.
[43] Lilie, H., Jaenicke, R. and Buchner, J. (1995) Protein Sci. 4, 917–924.
[44] Karlsson, R. (1994) Anal. Biochem. 221, 142–151.
[45] Nieba, L., Krebber, A. and Plückthun, A. (1996) Anal. Biochem. 234, 155–165.
[46] Hanes, J., Jermutus, L., Weber-Bornhauser, S., Bosshard, H.R. and Plückthun, A. (1998) Proc. Natl. Acad. Sci. USA 95, 14130–14135.
[47] Knappik, A. et al. (2000) J. Mol. Biol. 296, 57–86.
[48] Virnekäs, B., Ge, L., Plückthun, A., Schneider, K.C., Wellnhofer, G. and Moroney, S.E. (1994) Nucleic Acids Res. 22, 5600–5607.
[49] Kretzschmar, T. and von Rüden, T. (2002) Curr. Opin. Biotechnol. 13, 598–602.
[50] Barbas, C.F., Kang 3rd, A.S., Lerner, R.A. and Benkovic, S.J. (1991) Proc. Natl. Acad. Sci. USA 88, 7978–7982.
[51] Hoogenboom, H.R., de Bruine, A.P., Hufton, S.E., Hoet, R.M., Arends, J.W. and Roovers, R.C. (1998) Immunotechnology 4, 1–20.
[52] Marget, M. et al. (2000) Tissue Antigens 56, 1–9.
[53] Topping, K.P., Hough, V.C., Monson, J.R. and Greenman, J. (2000) Int. J. Oncol. 16, 187–195.
[54] Shadidi, M. and Sioud, M. (2001) Biochem. Biophys. Res. Commun. 280, 548–552.
[55] Sui, J., Bai, J., St Clair Tallarico, A., Xu, C. and Marasco, W.A. (2003) Eur. J. Biochem. 270, 4497–4506.
[56] Hoogenboom, H.R. et al. (1999) Eur. J. Biochem. 260, 774–784.
[57] Mutuberria, R., Hoogenboom, H.R., van der Linden, E., de Bruine, A.P. and Roovers, R.C. (1999) J. Immunol. Methods 231, 65–81.

[58] Jespersen, L.K., Kuusinen, A., Orellana, A., Keinanen, K. and Engberg, J. (2000) Eur. J. Biochem. 267, 1382–1389.
[59] Mirzabekov, T., Kontos, H., Farzan, M., Marasco, W. and Sodroski, J. (2000) Nat. Biotechnol. 18, 649–654.
[60] Dierks, T. and Krämer, R. (1988) Biochim. Biophys. Acta 937, 112–126.
[61] Jung, H., Tebbe, S., Schmid, R. and Jung, K. (1998) Biochemistry 37, 11083–11088.
[62] Knol, J., Sjollema, K. and Poolman, B. (1998) Biochemistry 37, 16410–16415.
[63] Gioannini, T.L., Howard, A.D., Hiller, J.M. and Simon, E.J. (1985) J. Biol. Chem. 260, 15117–15121.
[64] Tucker, J. and Grisshammer, R. (1996) Biochem. J. 317, 891–899.
[65] Callaghan, R., Berridge, G., Ferry, D.R. and Higgins, C.F. (1997) Biochim. Biophys. Acta 1328, 109–124.
[66] Mirzabekov, T., Bannert, N., Farzan, M., Hofmann, W., Kolchinsky, P., Wu, L., Wyatt, R. and Sodroski, J. (1999) J. Biol. Chem. 274, 28745–28750.
[67] Reich-Slotky, R., Panagiotidis, C., Reyes, M. and Shuman, H.A. (2000) J. Bacteriol. 182, 993–1000.
[68] Neumann, L., Wohland, T., Whelan, R.J., Zare, R.N. and Kobilka, B.K. (2002) Chembiochem 3, 993–998.
[69] Hoogenboom, H.R. (1997) Trends Biotechnol. 15, 62–70.
[70] Sheets, M.D. et al. (1998) Proc. Natl. Acad. Sci. USA 95, 6157–6162.
[71] Steinhauer, C., Wingren, C., Hager, A.C. and Borrebaeck, C.A. (2002) Biotechniques Suppl., 38–45.
[72] Venturi, M. and Hunte, C. (2003) Biochim. Biophys. Acta 1610, 46–50.
[73] Jung, S., Honegger, A. and Plückthun, A. (1999) J. Mol. Biol. 294, 163–180.
[74] Desiderio, A. et al. (2001) J. Mol. Biol. 310, 603–615.
[75] Ewert, S., Honegger, A. and Plückthun, A. (2003) Biochemistry 42, 1517–1528.